

# PROGRESS IN SIMULATIONS FOR SHORT AND LONG GLASS FIBER THERMOPLASTIC COMPOSITES

*Gregorio M. Vélez-García, Kevin Ortman, Neeraj Agarwal, Peter Wapperom, and Donald G. Baird, Virginia Tech, Blacksburg, VA*

## Abstract

We study fiber orientation in simple and complex flow geometries for highly concentrated short and long glass fiber suspensions. Three important aspects are the implementation of new theories to model fiber orientation, the evaluation of model parameters from rheological experiments, and an accurate simulation tool based on discontinuous Galerkin Finite element method. A delayed-fiber orientation evolution model, model parameters obtained by simple flow experiments, fiber orientation measured experimentally at the gate, and coupled simulations help to improve the prediction of short fiber orientation in a center-gated disk. In the case of long glass fiber, a Sliding Plate Rheometer (SPR) has been fabricated to acquire model parameters values for the use of the subsequent simulations of long glass fibers reinforced center-gated disks. In addition, a bead-rod model that accounts for the semi-flexible nature of the fibers is investigated to determine its feasibility for long glass fibers simulations.

## Introduction

Fiber reinforced thermoplastics made by injection molding are an attractive technology to develop lightweight, high-performance materials. These materials have generated lot of interest in automotive industry because of their excellent mechanical properties obtained in the final product, the high throughput, and low production cost. The desired properties are only obtained when the orientations of the particles coincide with the direction of mechanical interest. However, the fiber orientation varies through the part as a consequence of flow within the mold during the forming; a flow induced orientation. The physics behind the flow induced orientation get more complex as the fibers cross the threshold of 1 mm or  $a_r > 30$ . Fibers below this threshold value are considered as short fibers and they are assumed as rigid cylindrical objects. While fibers with length above the threshold value are classified as long glass fibers. The semi-flexibility due to the length is the main structural characteristic of the long fibers. The fibers considered in our research are either short or long glass fiber within a commercial range of concentration.

Optimization of the technology requires a prediction tool using a computer model capable of designing molding and processing conditions, the correct molding machinery, and consistently controlling fiber orientation. The actual capabilities of simulations in commercial software are only available for short glass fiber composites. However, they are unable to make a quantitative prediction of the orientation due to several limitations in the modeling and numerical techniques used to solve the system of equations. Some of the limitations in the approaches are the use of models that ignore the fiber interactions (Jeffery model<sup>1</sup>), or account for them in a concentration below the commercial interest (Folgar-Tucker model<sup>2</sup>), and use a decoupled approach to solve the system of equations. Much work has been accomplished in simulating the orientation of short glass fibers in polymeric melts, however relatively few efforts have produced applicable models that can be efficiently used to model long glass fiber orientation. This is, in part, due to the flexible nature of the long glass fibers, whereas short fibers can be assumed rigid.

Recently, a modified version of the Folgar-Tucker model has been used to simulate long glass fiber composites with limited success<sup>3</sup>.

The traditional modeling of fiber orientation has used complex flow experiments such as injection molding to determine model parameters. We have proposed here that obtaining these parameters using simpler flows e.g. simple shear flow experiments could provide us with better and more unbiased results. Recently, rheological<sup>4-8</sup> and injection molding<sup>9</sup> experiments in concentrated short glass fiber suspensions have shown that the most widely used model, the Folgar-Tucker model, predicts a too fast evolution of fiber orientation. Eberle et al.<sup>5</sup> used a non-objective model where the rate of rotation is scaled down using a non-affine constant determined from rheological experiments. This model incorporating non-affine motion, where its model parameters were determined by simple shear flow experiments, is used in this study to predict the flow-induced orientation for short glass fibers in a center-gated disk. This model will be referred to as non-affine Folgar-Tucker model. Same approach utilizing the simple shear flow experiments has been initiated to determine the model parameters for models used to simulate long glass fiber composite behavior. However the length of the fibers requires modification in the rheometer to be used.

For the short glass fiber composites, this paper develops a 2D solution where the flow and fiber orientation equations are coupled. In addition, the Hele-Shaw approximation is used to simplify the balance equations. The material behavior is modeled using the non-affine Folgar-Tucker model and a Newtonian model for the fibers and polymer matrix, respectively. The model parameters were determined from simple shear flow experiments. The objective is to develop an accurate numerical tool capable of improving the prediction of the flow-induced orientation for short glass fiber in a commercial range of concentrations using a coupled approach.

In the case of long glass fiber composites, we have two objectives. First, we want to understand fiber orientation of long glass fibers (> 1mm) in polymer melts and the associated rheology in well-defined simple shear flow. Specifically, we are interested in associating the rheological behavior of glass fiber reinforced polypropylene with the transient evolution of fiber orientation in simple shear in an effort to model fiber orientation in complex flow. Second, we explore several models, in a complex flow, that take the semi-flexible nature of long glass fibers into account. We then compare these to experimentally determined results.

## Theoretical Background

### Balance Equations

The conservation equations for isothermal flow and highly viscous fluids are described by

$$\underline{\nabla} \cdot \underline{v} = 0 \quad (1)$$

$$\underline{\nabla} \cdot (-p\underline{\delta} + \underline{T}) = \underline{0} \quad (2)$$

where  $\underline{\nabla}$  represents the gradient operator,  $\underline{v}$  the velocity,  $p$  the pressure,  $\underline{\delta}$  the identity matrix, and  $\underline{T}$  the extra stress tensor.

### Simplification of the Balance Equations for Short Glass Fiber

The Hele-Shaw approximation can be used to simplify the conservation equation based on the fact that the molded parts thickness is much smaller than the overall part dimension. When

a center-gated disk geometry as shown in Figure 1 is considered, the Hele-Shaw flow approximation is described by

$$\frac{1}{r} \frac{\partial}{\partial r} (hr \bar{v}_r) = 0 \quad (3)$$

$$-\frac{\partial p}{\partial r} + \frac{\partial T_{rz}}{\partial z} = 0 \quad (4)$$

where  $r$  represents the radial or flow direction,  $z$  the gapwise direction,  $h$  the half gap width,  $\bar{v}_r$  the average radial velocity along the gapwise coordinate,  $p$  the pressure, and  $T_{rz}$  the shear component of the extra-stress tensor. These equations are supplemented by the typical boundary conditions for pressure and velocity<sup>10</sup>. The flow is assumed to be symmetrical in the angular direction,  $\theta$ .

### Simplification of the Balance Equations for Long Glass Fiber

The flow field is assumed to be uncoupled from the fiber orientation dynamics and can therefore be solved analytically<sup>10</sup> for cylindrical coordinates:

$$v_r(r, z) = \frac{3Q}{8\pi hr} \left[ 1 - \left( \frac{z}{h} \right)^2 \right] \quad (5)$$

$$v_z(r, z) = 0 \quad (6)$$

where  $Q$  is the volumetric flow rate.

### Orientation Equation for Short Glass Fibers

The orientation evolution tensor described by non-affine Folgar-Tucker model combines the Jeffery model, isotropic diffusion term, and a non-affine motion behavior. The non-deviatoric form of the model in a Newtonian solvent is described by

$$\frac{D\underline{\underline{A}}}{Dt} = \frac{\partial \underline{\underline{A}}}{\partial t} + \underline{\underline{v}} \cdot \nabla \underline{\underline{A}} = \alpha \left[ \nabla \underline{\underline{v}}^T \cdot \underline{\underline{A}} + \underline{\underline{A}} \cdot \nabla \underline{\underline{v}} - 2\underline{\underline{D}} : \underline{\underline{R}}_4 - 6C_I I \left( \underline{\underline{A}} - \frac{1}{3} \underline{\underline{\delta}} \right) \right] \quad (7)$$

where  $\underline{\underline{A}}$  and  $\underline{\underline{R}}_4$  represent the second order and fourth non-deviatoric orientation tensors, respectively. The first three terms inside the square parenthesis denote the kinematic contribution to the orientation while the fourth term represents and semi-dilute-regime interaction.  $\alpha$  is the non-affine constant, which is a time-delayed constant used to describe the multi-particle interactions in a concentrated suspension seen as a slowing down process of

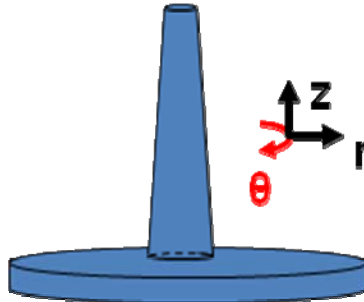


Figure 1: Center-gated disk geometry.

orientation.  $C_i$  is the interaction coefficient,  $\|\underline{\underline{D}}\|$  the magnitude of the rate of deformation tensor, and  $\underline{\underline{D}}$  the rate of deformation tensor.  $R_4$  can be approximated in terms of a quadratic closure

$$R_4 = \underline{\underline{A}}\underline{\underline{A}} \quad (8)$$

The non-affine Folgar-Tucker model described by Eq. (7) is a non-objective model but the simplification introduced by the Hele-Shaw approximation allows us to use the model to predict the flow-induced orientation in the center-gated disk flow.

### Orientation Equation for Long Glass Fibers

The fiber orientation for long glass fibers will be predicted using a model that explicitly introduces the semi-flexibility for dilute solutions using Bead-Rod analogy<sup>11</sup>. This Bead-Rod model is a continuum model that provides a first approximation to flexibility. This is accomplished by modeling a fiber as two rods connected by a pivot allowing bead (Figure 2). The model constructs two rigid segments with length  $l_B$  that are allowed to slightly pivot about the connecting bead, with some restorative bending rigidity. Both  $\vec{p}$  and  $\vec{q}$  are unit vectors that represent the orientation of the corresponding fiber segments, with respect to the center bead. Two orientation tensors representing the second moment of the distribution function of the unit vectors,  $\vec{p}$  and  $\vec{q}$ , are defined as:

$$\underline{\underline{A}} = \oint \vec{p}\vec{p}\psi(\vec{p},\vec{q})d\vec{p}d\vec{q} \quad (9)$$

$$\underline{\underline{B}} = \oint \vec{q}\vec{q}\psi(\vec{p},\vec{q})d\vec{p}d\vec{q} \quad (10)$$

The model proposed is given in Equations 13-17,

$$\frac{D\underline{\underline{A}}}{Dt} = \underline{\underline{\nabla v}}^T \cdot \underline{\underline{A}} + \underline{\underline{A}} \cdot \underline{\underline{\nabla v}} - 2\underline{\underline{D}} : R_4 + \frac{l_B}{2} [\underline{\underline{C}}\underline{\underline{\mu}} + \underline{\underline{\mu}}\underline{\underline{C}} - 2(\underline{\underline{\mu}} \cdot \underline{\underline{C}})\underline{\underline{A}}] - 2k[\underline{\underline{B}} - \underline{\underline{A}}tr(\underline{\underline{B}})] \quad (11)$$

$$\frac{D\underline{\underline{B}}}{Dt} = \underline{\underline{\nabla v}}^T \cdot \underline{\underline{A}} + \underline{\underline{A}} \cdot \underline{\underline{\nabla v}} - 2\underline{\underline{D}} : R_4 + \frac{l_B}{2} [\underline{\underline{C}}\underline{\underline{\mu}} + \underline{\underline{\mu}}\underline{\underline{C}} - 2(\underline{\underline{\mu}} \cdot \underline{\underline{C}})\underline{\underline{A}}] - 2k[\underline{\underline{A}} - \underline{\underline{B}}tr(\underline{\underline{B}})] \quad (12)$$

$$\frac{D\underline{\underline{C}}}{Dt} = \underline{\underline{\nabla v}}^T \cdot \underline{\underline{C}} - (\underline{\underline{A}} : \underline{\underline{\nabla v}}^T)\underline{\underline{C}} + \frac{l_B}{2} [\underline{\underline{\mu}} - \underline{\underline{C}}(\underline{\underline{\mu}} \cdot \underline{\underline{C}})] - \underline{\underline{\nabla v}}^T \underline{\underline{C}} [1 - tr(\underline{\underline{B}})] \quad (13)$$

$$\underline{\underline{\mu}} = \sum_{i=1}^3 \left( \sum_{j=1}^3 \sum_{k=1}^3 \frac{\partial v_i}{\partial x_j \partial x_k} A_{jk} \right) \mathbf{e}_i \quad (14)$$

where  $\underline{\underline{F}}$  represent the flexibility contribution. As a direct consequence to the bending rigidity, encompassed within the model parameter  $k$ , the expectancy of a segment orientation (with respect to the orientation distribution function) may be non-zero in general, and is accounted in

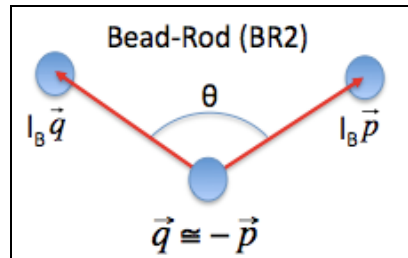


Figure 2: Fiber model, with segment length  $l_B$ , allowing semi-flexibility.

Equation 15 by the following definition:

$$\underline{\underline{C}} = \oint \bar{p}\psi(\underline{p}, \bar{p})d\bar{p}d\bar{q} \quad (15)$$

Lastly, Equation 14 contributes second order derivatives of the velocity field, with components  $v_i$ , that originate from a Taylor series approximation applied to the bead kinematics. In simple shear flow, for example, all components are 0. This vector, in Equation 14 is formed by the unit dyads  $\vec{e}_i$ .

## Constitutive Equations

The extra stress tensor for a fiber-filled polymeric suspension consists of two components

$$\underline{\underline{T}} = \underline{\underline{T}}^{fibers} + \underline{\underline{T}}^{matrix} \quad (16)$$

where  $\underline{\underline{T}}^{fibers}$  is the stress due to the short glass fibers in the fluid and  $\underline{\underline{T}}^{matrix}$  is the contribution of the polymer matrix. The extra stress tensor contribution due to the matrix depends on the behavior of the polymer used as solvent. For matrices behaving like a Newtonian fluid, the Newtonian constitutive equation can be used to describe the polymer. It has the form

$$\underline{\underline{T}}^{matrix} = 2\eta\underline{\underline{D}} \quad (17)$$

where  $\eta$  is the Newtonian viscosity. The extra stress contribution of the short glass fibers can be modeled as

$$\underline{\underline{T}}^{fibers} = \nu\zeta_{str}\underline{\underline{D}} : \underline{\underline{R}}_4 \quad (18)$$

where  $\nu$  denotes the particle concentration.  $\zeta_{str}$  represents the viscous drag coefficient. In decoupled flow and fiber orientation simulations the extra stress contribution of the long glass fiber  $\underline{\underline{T}}^{fibers}$  is set to 0.

## Experimental Methods

### Rheology of Short Glass Fiber Suspension

The material parameters were determined from steady shear and start-up of shear experiments using a cone-and-plate rheometer (CPR)<sup>6</sup>. Over a wide range of shear rates the PBT matrix behaves like a Newtonian fluid with viscosity  $\eta = 426$  Pa·s. The particle parameters were determined as  $\nu\zeta_{str} = 5000$  Pa·s and  $C_l = 0.02$ . The weighted average length of the fiber was 364  $\mu\text{m}$ .

### Rheology of Long Glass Fiber Suspension

Rheological measurements of long glass fiber composites with instruments like rotational and capillary rheometers present severe experimental problems such as inhomogeneous flow fields and excessive fiber breakage. To overcome these problems, a Sliding Plate Rheometer (SPR) incorporating a Wall Shear Stress Transducer is designed and fabricated. It presents various advantages over other standard rheometers. For example, it gives localized stress measurement and induces homogenous shear field with rectilinear stream lines which made it a much more suitable device to study the fiber filled systems. To validate the behavior of this newly fabricated instrument, it is tested with different materials which exhibit well defined rheological behavior. Two test materials used here are polydimethylsiloxane (PDMS), a high viscosity Newtonian fluid and Equistar PETROTHENE NA-952, a low density Polyethylene (LDPE) with no processing aids or antiblock agents.

Moreover, in order to validate the behavior of SPR for fiber filled suspensions, it is tested with short fiber composite. Stress growth tests are conducted using 30 wt % short glass fiber

filled polypropylene. The molecular weight of this resin was found to be low. Results obtained from the SPR are compared with the similar results obtained from cone and plate rheometer. Samples for both SPR and CPR are manufactured such that fibers are nearly randomly oriented in the plane of motion before the start of the test. In CPR, to remove the inevitable fiber-boundary interaction near the center, sample disks are pre-formed and a 25.4 mm diameter hole is drilled through the center creating a donut shaped sample. Shear rate in these experiments is varied from  $0.1 \text{ s}^{-1}$  to  $1.5 \text{ s}^{-1}$ .

### **Injection Molding Experiments**

A 75% short shot center-gated disk of 30 wt% short glass fiber PBT with internal radius ( $r_i$ ) of 2.98 mm, outer radius ( $R$ ) of 30.81 mm, and thickness ( $2h$ ) of 1.31 mm was used. In the case of long glass fiber composites the suspension contained 40 wt% long glass fiber PP. The outer diameter was approximately 53 and the thickness 2.05 mm. The initial length of long glass fiber specified by the resin provider was 11 mm. The filling time of the part was approximately 1 s and the injection pressure was estimated to be 20 MPa.

### **Fiber Orientation in Center-gated Disks**

The initial orientations of the fibers were experimentally determined at the gate using the method of ellipses<sup>6</sup> from optical-reflection micrographs taken on a metallographically polished surface in  $r,z$ -planes. The samples were cut along a line of constant  $\theta$ . The initial orientation tensor  $\mathbf{A}$  was computed using a weighted average of orientations of all individual particles within rectangles of dimension  $h/6$  in  $z$ -direction and  $h/3$  in  $r$ -direction. For validation purposes the orientation was determined in a similar manner along the gapwise direction at 40% and 90% of  $(R-r_i)$ .

## **Numerical Methods**

In the simulations dealing with short glass fiber composites, the standard Galerkin finite element method (GFEM) is used in the discretization of the HS flow approximation of the balance equations. While in the simulation related to long glass fiber the analytical solution was computed. The discontinuous Galerkin finite element method (DGFEM) with a standard explicit Euler scheme is used to discretize the evolution equations. In the simulations only the top half of the domain was considered with no slip velocity at the wall and symmetry boundary conditions at  $z=0$ .

## **Discussion**

### **Experimental Orientation for Short Glass Fiber Center-Gated Disk**

A limited amount of studies exist in the literature that combines an experimental and numerical program. Typically a random initial orientation condition along the thickness is assumed, especially for a center-gated disk. That means a plug-like profile for the orientation component as shown in Figure 3(a). However, the orientation determined experimentally from a 75% short shot center-gated disk shown in Figure 3(b) reveals an asymmetric profile at the gate region. This result corroborates predictions indicated in the literature but never validated<sup>12, 13</sup>. The experimental results in Figure 3(b) also show that the values of orientation components are far from random orientation, especially for the  $A_{zz}$  components.

The orientation along the thickness measured at 40% and 90%  $(R-r_i)$  for PBT filled with short glass fiber indicates changes in the magnitude and distribution of the orientation

components compared to the orientation at the gate. Figure 4 shows the experimental evolution of the orientation for the  $A_{rr}$  orientation components in the gate, 40% and 90% ( $R-r_i$ ). The initial asymmetry fades as the function of the radial location, but still is present at regions close to the end of flow for the center-gated disk used in the experiments. However, the experimental results suggest the development of a symmetric orientation or stable structure of orientation for disks of larger diameter as described by Rao and Altan<sup>14</sup>.

### Prediction of Orientation for Short Glass Fibers Center-gated Disk

The predicted evolution of orientation in the cavity is influenced by the asymmetric orientation at the gate and the simulation strategy, i.e, coupled or decoupled approach. Indeed, the initial orientation affects local values of orientation while the solution strategy affects the velocity of orientation evolution prediction. Figures 5 (a) and (b) show decoupled simulation results for the radial locations of 40% and 90% ( $R-r_i$ ), respectively, focused on the upper half cavity. These predictions (lines) overestimate the  $A_{rr}$  orientation components while they underestimate the  $A_{\theta\theta}$  and  $A_{rz}$  orientation components, when compared to the experimental results (symbols). The smooth predicted profile cannot reproduce a series of peaks and valleys observed in the experimental profile of orientation. These features in the orientation profile can be related to the layered structure formed at the gate, which evolves locally as the flow progresses<sup>15</sup>. This may imply that the decoupled simulation using the non-affine Folgar-Tucker model is evolving faster than the experimental evolution of orientation.

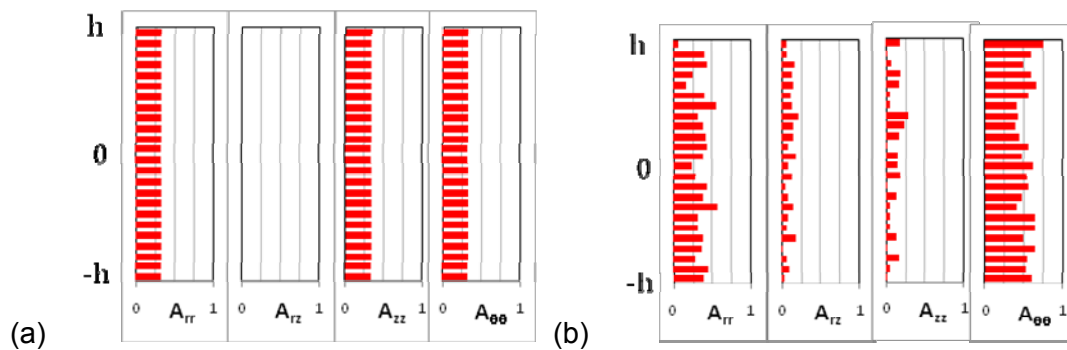


Figure 3. Experimental values of  $A_{ij}$  along the cavity thickness (a) at the gate and (b) close to the end of fill (90% of radial flow length).

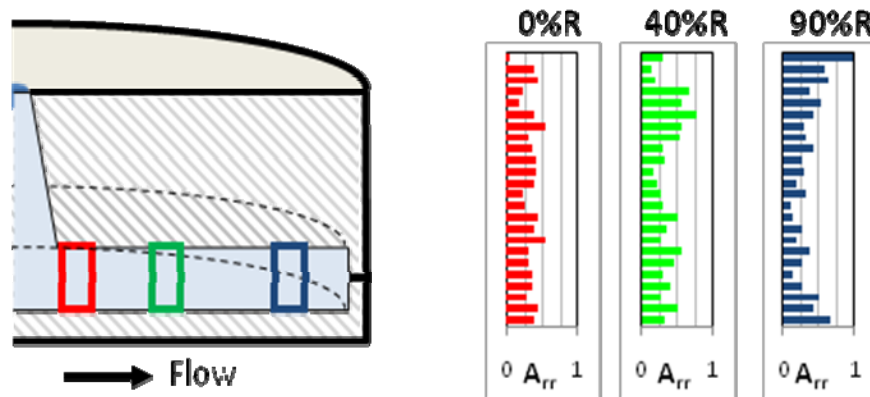


Figure 4. Experimental values of  $A_{rr}$  along the cavity thickness at three radial locations: gate, 40% ( $R-r_i$ ), and 90% ( $R-r_i$ ).

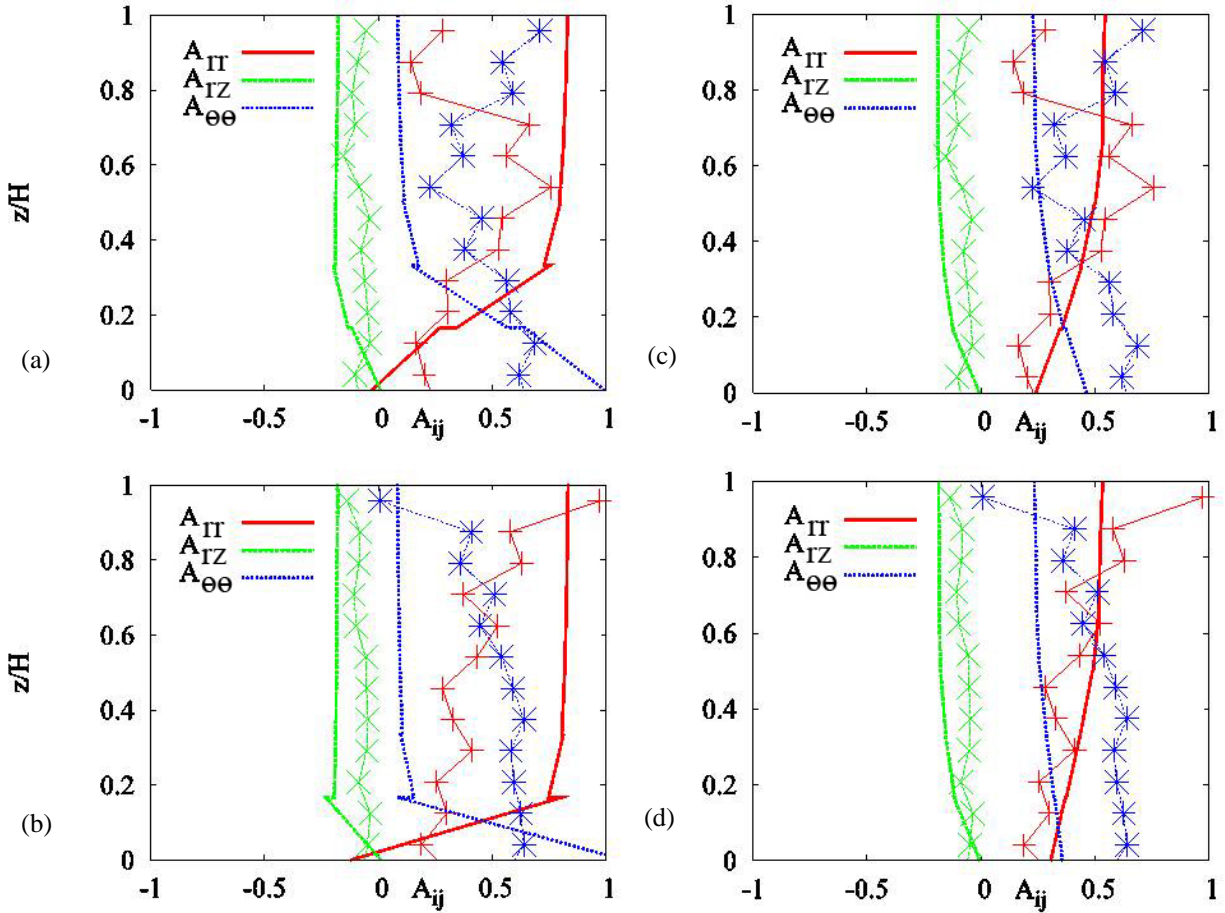


Figure 5. Experimental and predicted orientations from decoupled simulation at (a) 40% ( $R-r_i$ ) and (b) 90% ( $R-r_i$ ) and from coupled simulations at (c) 40% ( $R-r_i$ ) and (d) 90% ( $R-r_i$ ). The dimensionless simulation time was 290. The lines denote the predictions, while the symbols are used to indicate the experimental results.

The results of the coupled simulation show improvement in the prediction of the orientation profile. Figure 5 depicts for (c) 40% ( $R-r_i$ ), and (d) 90% ( $R-r_i$ ). The results are sensitive to the use of the non-affine Folgar-Tucker model because the retardation of evolution considerably improves the prediction of  $A_{rr}$ , but the profile of the predicted orientation is smooth. In general the  $A_{\theta\theta}$  is underestimated, but not as severely as in the decoupled approach. An interesting observation in coupled simulations is that the difference between experimental and predicted  $A_{\theta\theta}$  is greater at 90% ( $R-r_i$ ) than at 40% ( $R-r_i$ ). This can be an effect of using the Hele-Shaw approximation, because this simplification ignores the existence of the flow front. It is well known that the front is a region dominated by extensional flow which is the driving mechanism for  $A_{\theta\theta}$ . Therefore, these coupled results suggest the need for full simulations, which are especially important in small geometries where the evolution of orientation never reaches the steady structure of orientation.

### Prediction of Orientation for Long Glass Fibers Center-gated Disk

For both the Folgar-Tucker model and the Bead-Rod model a random initial orientation at the gate was specified. The model parameter  $k$  was set equal to a dimensionless value of 0.5.<sup>11</sup> Additionally, the segment length  $l_B$  was given a dimensionless value that approximately corresponds to 0.5 mm; however fiber attrition data may be needed for accuracy. The

numerical results for the Bead-Rod model and experimental data are given in Figure 6, and those for the Folgar-Tucker model are given in Figure 7.

The Bead-Rod simulation predicts a much broader orientation distribution, as compared to what was obtained using the Folgar-Tucker model. Although the qualitative behavior of the orientation is better represented in this figure (especially for  $A_{11}$ ), the results for  $A_{33}$  and  $A_{22}$  are different from what is observed experimentally. The simulation results with the Bead Rod model are therefore also not satisfactory in comparison with the results obtained experimentally. It should, however, be noted that the parameters available within this model should be more precisely determined, and/or fit, before full judgment of this model may be passed. This will therefore become the nature of future work.

To further explore the effects of flexibility, the Bead-Rod model and the Folgar-Tucker model were used in the startup of steady shear flow for a fiber suspension that was random in the shear plane. Figure 8 shows that the flexibility parameter may be directly used to delay the transient behavior, thus capturing behavior more true to what is obtained experimentally.

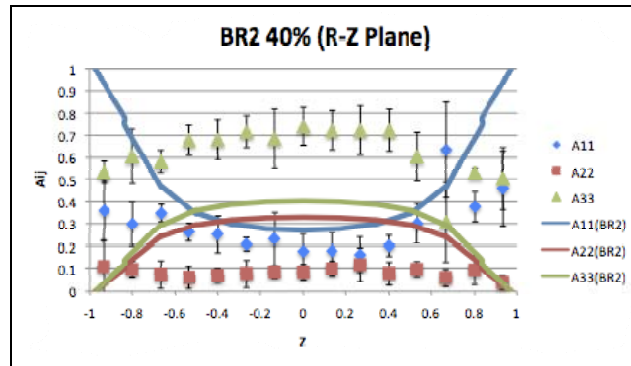


Figure 6: Bead-Rod (BR2) simulation and experimentally measured results, for the trace components of the orientation tensor, versus the dimensionless mold thickness. The components are give by “ $r = 1$ ”, “ $z = 2$ ”, “ $\theta = 3$ .”

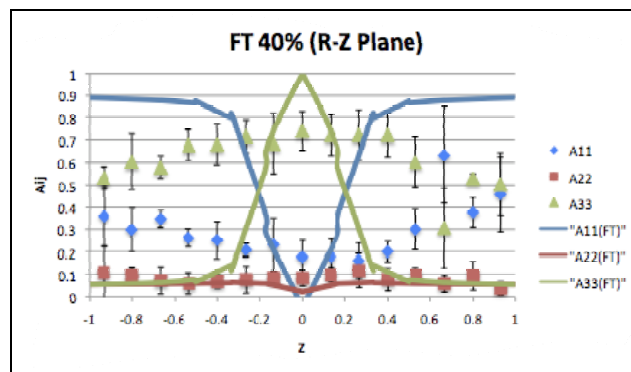


Figure 7: Folgar-Tucker (FT) simulation and experimentally measured results, for the trace components of the orientation tensor, versus the dimensionless mold thickness. The components are give by “ $r = 1$ ”, “ $z = 2$ ”, “ $\theta = 3$ .”

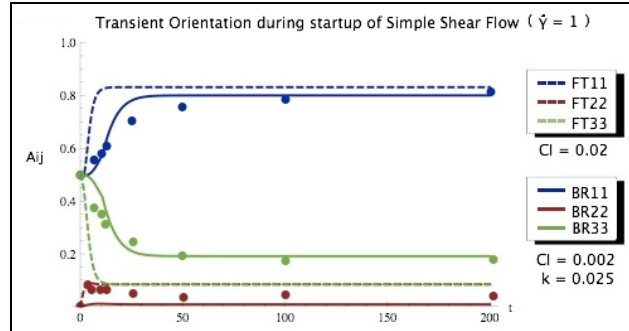


Figure 8: Transient evolution of fiber orientation during the startup of steady shear flow.

## Rheology of Long Glass Fiber Suspension

Stress growth curves obtained for high viscosity PDMS and NA 952 at different shear rates using SPR matched perfectly with similar curves obtained from the conventional rheometers. This ensures that the fabricated SPR can be used to generate meaningful rheological data for simple shear experiments. In the case of short glass fiber composites, stress growth curves were obtained for four different shear rates 0.1, 0.5, 1.0, and 1.3  $s^{-1}$ . For all these shear rates results for SPR and CPR were quite consistent with each other. Figure 9 depicts one of these results at shear rate 0.5  $s^{-1}$ . These results are produced more than once to check the reproducibility of the fabricated SPR and deviation was found to be less than 8%, which is acceptable for fiber filled systems.

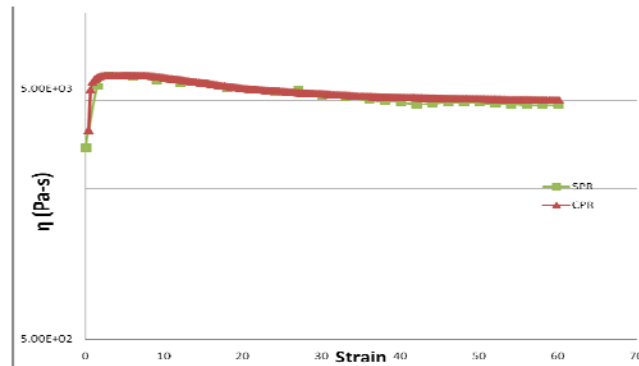


Figure 9: Shear Viscosity Growth Curve for Short Glass Composites at Shear Rate 0.5  $s^{-1}$ .

## Conclusions

A 2D coupled method for predicting the flow-induced orientation of short glass fibers in thin walled injection molded composite parts has been presented. The impact of inter-particle interactions and the orientation at the gate was investigated using parameters determined from rheometry. Our experimental results indicate that the profile of orientation at the gate cannot be assumed to be random for a center-gated disk. In addition, the orientation transient remains through the geometry. Results indicate that the non-affine Folgar-Tucker model is not able to retard the orientation evolution in decoupled simulations. However, the coupled simulations improve the prediction of  $A_{rr}$  components and suggest the need for simulations considering the frontal flow region.

Long fiber kinematics, in complex flow, is not accurately explained by the Folgar-Tucker or the Bead Rod models and/or the assumptions used in the simulation of these models. One

solution to this would be to more accurately determine and/or fit parameters for the Bead Rod model (as was done with the Folgar Tucker model) and use initially determined orientations within the simulations. This would ensure that these particular models are functioning most properly. If indeed these efforts still produce less than convincing results, the next step may be to first try to understand long fiber behavior in simple flow (rather than complex) by using well defined flows to study the desired behavior. Additionally, well-defined flows may be utilized to obtain rheological data, from which parameter data may be obtained. It is thus believed that studying long fibers in simple flow will provide a more fundamental opportunity to understand their behavior.

Specifically, a sliding plate rheometer that we believe is capable of conducting such simple flow studies on long glass fibers, given the advantages it has over conventional devices, has been fabricated and validated. From the results obtained using various materials including fiber filled systems, following can be concluded for the SPR. First, this device is capable of generating unbiased and reproducible rheological data irrespective of its simple design, and second, it can be used for the transient rheological measurements of fiber filled systems including long glass fiber composites.

## Acknowledgements

The financial support of NSF/DOE: DMI-052918 is gratefully acknowledged. Gregorio M. Vélez-García also acknowledges support from MS&IE-IGERT, University of Puerto Rico-Mayagüez. The authors also would like to thank the undergraduate students Eric B. Webb and Johnny Rokisky, who contributed to the experimental portion of this study.

## References

1. Jeffery, G. B., *Proc. R. Soc. A* **1922**, *102*, 161-179.
2. Folgar, F. P., Tucker, C.L., *J Reinf Plast Comp* **1984**, *3*, 98-119.
3. Phelps, J. H., Tucker, C.L., *J. Non-Newtonian Fluid Mech.* **2009**, *156*, 165-176.
4. Sepehr, M., Ausias, G., Carreau, P.J., *J. Non-Newtonian Fluid Mech.* **2004**, *123*, 19-32.
5. Eberle, A. P. R., Vélez-García, G M., Baird, D.G., Wapperom, P., *J Non-Newtonian Fluid Mech Submitted*.
6. Eberle, A. P. R., Baird, D.G., Wapperom, P., Vélez-García, G M., *J Rheol Submitted*.
7. Eberle, A. P. R., Baird, D.G., Wapperom, P., Vélez-García, G M., *J Rheol Submitted*.
8. Sepehr, M., Carreau, P.J., Grmela, M., Ausias, G., Lafleur, P.G., *J Polym Eng* **2004**, *24* (6), 579-607.
9. Huynh, H. M. Improved fiber orientation predictions for injection-molded composites. University of Illinois at Urbana-Champaign, 2001.
10. Baird, D. G., Collias, D.I., *Polymer processing: Principles and design*. Wiley, John & Sons, Incorporated: 1998.
11. Strautins, U., Latz, A., *Rheol Acta* **2007**, *46*, 1057-1064.
12. VerWeyst, B. E., Tucker, C. L., *Can J Chem Eng* **2002**, *80*, 1093-1106.
13. Chung, D., Kwon, TH, *J. Non-Newtonian Fluid Mech.* **2002**, *107*, 67-96.
14. Altan, M. C., Rao, B. N., *J Rheol* **1995**, *39* (3).
15. Vélez-García, G. M., Ortman, K., Eberle, A. P. R., Wapperom, P., Baird, D. G. In *Simulation of orientation in injection molding of high aspect ratio particle thermoplastic composites*, Proceedings of the XVth International Congress of Rheology, Monterey, CA, August 3-8; Monterey, CA, 2008.